ACADEMIC PRESS

Available online at www.sciencedirect.com

SCIENCE DIRECT®

Journal of Sound and Vibration 263 (2003) 153–174

JOURNAL OF SOUND AND VIBRATION

www.elsevier.com/locate/jsvi

Acoustical analysis of pipes with flow using invariant field functions

G. Pavić*

Laboratoire Vibrations-Acoustique, Institut National des Sciences Appliquées de Lyon, 20, Avenue Albert Einstein, 69621 Villeurbanne, France

Received 16 October 2001; accepted 3 May 2002

Abstract

An analysis of the pressure field within a pipe is carried out using simplified formulations of pipe acoustics. The fluid contained within the pipe is considered non-viscous, while the flow velocity of the fluid is assumed to be smaller than the speed of sound.

The analysis is limited to frequencies which are well below the pipe ring frequency, i.e., at which only simple waves can propagate. Expressions and diagrams are given which specify the applicable frequency range in each particular case.

Three invariant functions of the internal pressure field are evaluated. These functions allow for the determination of the following quantities: base pressure spectrum (spatial mean r.m.s. value), lower and upper bounds of the pressure spectrum for the entire pipe, pressure spectrum at an arbitrary position, speed of sound in the contained fluid and fluid flow velocity.

Experimental identification of these quantities requires simultaneous measurement at three points. A few measurements carried out on one air-filled and one water-filled pipe have demonstrated the potential of pipe invariant functions for acoustical analysis.

1. Introduction

At lower frequencies, well below the ring frequency of the pipe, pipe vibrations are similar to that of a beam of deformable cross-section which not only can move in flexure but also axially and can expand in radius. If the fluid within the pipe is heavy, coupling between the fluid and the pipe wall can affect vibration even at low frequencies. In order to analyze pipe vibration and fluid pressure pulsations in a meaningful way, use of a pipe model in more detail than that of a beam

*Corresponding author. Tel.: +33-4-72438707; fax: +33-4-72438712.
E-mail address: pavic@lva.insa-lyon.fr (G. Pavić).

0022-460X/03/$ - see front matter
PII: S0022-460X(02)01102-1

becomes necessary. Such a model can fulfil two roles: produce results closer to reality but also set limits to the range of lower frequencies within which the pipe acoustics is still simple enough to allow not too demanding experimental analysis.

The model used here is that of a fluid-filled circular cylindrical shell, being the closest known model of a deformable waveguide. Using the exact expressions for pipe motion from this model, low-frequency simplifications will be made. It should be pointed out that the exact expressions of pipe vibration and the resulting simplified ones will be obtained on the basis of the so-called thin-wall theory. Most of the smaller pipes have thickness-to-diameter ratios above the thin-wall theory limit. However, this will not appear as a drawback in the present analysis, as the effects restricting the results will apply to very thin pipes only. In particular, the limitations of the simple pipe behaviour which are applicable to frequencies much lower than the ring frequency will intrinsically not apply to thick pipes.

The acoustics of circular cylindrical shells has been analyzed by a number of researchers. Basic notions of fluid–structure interaction in cylindrical shells can be found in Refs. [1,2]. A detailed account of vibracoustics of fluid-filled shells was given by Fuller and Fahy [3], as well as by Möser et al. [4]. Thorough explanations were made about the nature of different waves and the evolution from one type to another with frequency. An original method was used by Bobrovnitskii and Tyutekhin in Ref. [5] to compute the shell wave characteristics, using a distributed impedance concept to account for the coupling. An alternative method was employed by the author [6], using polynomial expansion of the fluid loading function for computing the wave characteristics and energy flow.

The techniques used in Refs. [3–6] enable an exact computation to be made of the dispersion law for a fluid-filled pipe which sets grounds for the development of comprehensive measurement techniques.

Verheij has demonstrated that simple measurements on fluid-filled pipes are feasible under certain conditions where basic pipe motions are separable to allow individual treatment of different wave types, [7,8]. In Ref. [9] an approach was presented where unseparable motions could be treated. Bourget and Fahy discussed multi-transducer measurements in Ref. [10] adapted to complex vibrational behaviour of cylindrical shells at higher frequencies. Some original measurement techniques were further reported by de Jong and Verheij [11,12] and later by Trdak [13], which account for simultaneous propagation of different modes of vibration. By analyzing pipe vibration from the point of noise radiation Feng has found that the pulsatory pipe motion can be an efficient sound radiator [14]. The same author has carried out measurements of higher order waves using a technique similar to that of Bourget and Fahy [15]. In Ref. [16] this author has outlined some practical techniques for the analysis of pressure pulsations in pipes of small diameter.

The analysis which follows concerns pressure fluctuations in a straight fluid-filled pipe. Both the pipe wall and the contained fluid are assumed lossless. Although not strictly valid, this assumption will cause inaccuracies of second order only, but will in turn simplify the analysis considerably. The flow speed is taken into account, but is considered to be much smaller than the speed of sound in either the fluid or the pipe material. The pressure fluctuations are of prime concern. These are supposed to originate from hydraulic sources, such as pumps in regular operation, which create pressure waves of plane wave type uncontaminated by cavitation or flow-generated turbulence.

2. Theoretical background

Pressure pulsations propagate in pipes at a speed which is lower than that in an infinite medium. The decrease of speed of sound is an effect of fluid coupling with the motion of the pipe wall. A rigorous analysis of pressure pulsation has to take coupling into account. This will be made here by taking the full series development of the pressure field and later simplify this representation by keeping only the lower order terms which adequately describe this field at lower frequencies.

The pipe will be considered as a cylindrical circular shell specified by its outer diameter D and thickness h as well as material properties: Young's modulus E, mass density ρ_s and the Poisson ratio υ. The fluid within the pipe is characterized by its mass density ρ_f and speed of sound $c_{f\infty}$, the symbol ∞ implying the speed in the unbounded fluid.

2.1. Exact solution of pipe vibration

The exact solution will be briefly recalled in this section as it will be required later as the basis for a simplified one. The exact solution used here is based on thin-wall theory of a vibrating cylindrical shell which satisfies Kirchhoff's assumptions on the linearized displacement distribution across the wall thickness. Several differential shell operators have been developed around this theory, see e.g., Ref. [17]. The one by Flügge [18] will be used in the present analysis.

During vibration the pipe cross-section deforms. Any deformation can be decomposed into harmonic components of circumferential orders $n = 0, 1, 2\ldots$. Of particular importance for pipes are the deformations of the order $n = 0$, called the "breathing mode", and that of the order $n = 1$, the "flexural mode". To each order n there correspond a number, theoretically infinite, of distinct axial wave numbers. These can be real, imaginary or complex thus representing propagating, evanescent or quasi-propagating waves, respectively. The latter are similar to propagating waves but with a decaying amplitude. The global pipe motion in a general case will be a superposition of different waves.

The radian frequency and the wave number are usually put in a non-dimensional form, the former by dividing it by the pipe ring frequency $c_{s\infty}/a$, the latter by multiplication by the mean pipe radius a:

$$\Omega = \frac{\omega a}{c_{s\infty}}, \quad \kappa = ka \quad \text{where } a = (D-h)/2, c_{s\infty} = \sqrt{\frac{E}{\rho_s(1-\upsilon^2)}}; \tag{1}$$

$c_{s\infty}$ is the speed of sound in the unbounded sheet of pipe material, E is Young's modulus and ρ_s is the mass density of the pipe material.

It has been found [3,4] that only a few waves of orders $n = 0$ and 1 can propagate in fluid-filled shells well below its ring frequency, $\Omega \ll 1$, all other waves being of decaying type. Propagating waves include two types of plane waves and torsional waves—all of order $n = 0$—as well as flexural waves, of order $n = 1$. Torsional waves of order $n = 0$, the only ones which do not couple wall vibration to fluid motion, will be not analyzed here in view of their limited importance in pipe acoustics. Each wave, apart from the torsional one, propagates in both the fluid and the pipe wall at the same wavelength due to coupling. Waves of orders $n > 1$, called higher order waves, can propagate only above a certain cut-on frequency. This frequency, depending on pipe diameter, thickness, wall parameters and fluid parameters, increases with wave order n.

Fig. 1 shows a few lowest wave numbers corresponding to order $n=0$ for a water-filled steel pipe with thickness-to-diameter ratio $\frac{1}{40}$ (left) and $\frac{1}{10}$ (right). The two types of plane waves which can propagate from zero frequency are of different wave numbers. One of higher wave number will be termed "fluid wave" as its energy is predominantly contained in the fluid. The other one will be termed "longitudinal wave" as its energy is predominantly contained in the pipe wall exhibiting axial motions. These two waves are the subject of the present investigation. The terms fluid and longitudinal are certainly not optimal in the strict sense, but can facilitate the distinction between the two as other waves will not be analyzed.

The first higher wave will cut on at $\Omega \approx 0.8$ and 0.9 in the two cases displayed. The evanescent waves, presented by thin lines, are of relatively high wave number, i.e., these waves decay rapidly. So do the quasi-propagating waves, where the imaginary part of the wave number, responsible for spatial attenuation, is represented by dotted lines (only one is seen in the actual figure, the others being higher up). All of this means that, providing the frequency stays moderately low, the fluid and the longitudinal waves are of sole concern where the mode $n = 0$ is concerned.

Fig. 2 shows the wave numbers for the pipe of thickness-to-diameter ratio $\frac{1}{40}$, corresponding to orders $n = 1-6$. Orders higher than 1 have non-zero cut-on frequencies which rise with the order number. Above the cut on all orders exhibit approximately square-root of frequency dependence only to deviate at higher frequencies from this law. Evanescent and quasi-propagating waves for orders $n > 1$ are unimportant at frequencies lower than the corresponding cut-on frequency as the imaginary part of the wave number of these stays high. Consequently, at low frequencies up to the cut on of the order $n = 2$, only the flexural evanescent waves are of practical importance as these are of rather small wave number extending down to zero frequency.

At or close to cut-on frequencies, the imaginary part of the wave number of evanescent or quasi-propagating waves becomes small implying that the penetration depth of these waves increases well beyond the immediate vicinity of pipe ends or excitation points.

The limit of simple pipe behaviour where only breathing mode is concerned, $n = 0$, is the first non-zero cut-on frequency of this mode.

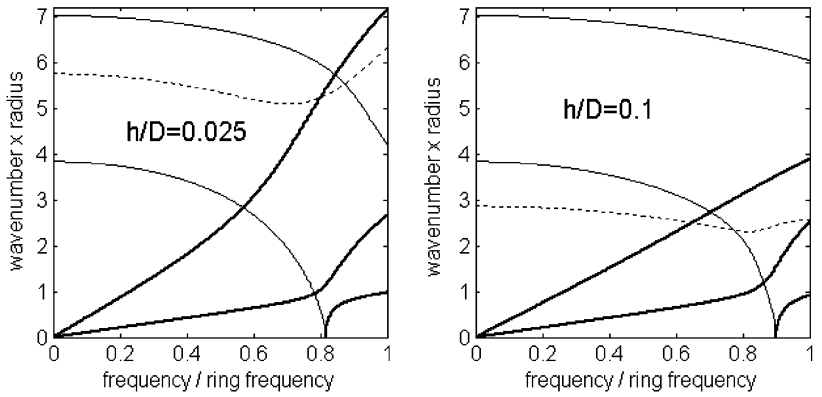

Fig. 1. Wave number diagram for a water-filled steel pipe: order $n = 0$. Thickness/diameter: $\frac{1}{40}$ (left), $\frac{1}{10}$ (right). Thick line: propagating waves, thin line: evanescent waves, dotted line: quasi-propagating waves—imaginary part.

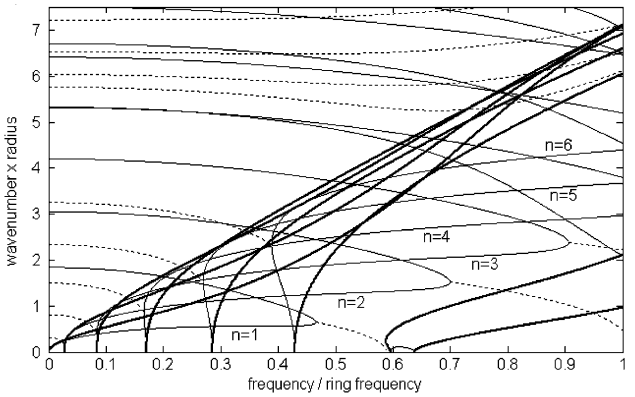

Fig. 2. Wavenumber diagram for a water-filled steel pipe: orders $n = 1-6$. Thickness/diameter $= \frac{1}{40}$. Thick line: propagating waves, thin line: evanescent waves, dotted line: quasi-propagating waves—imaginary part. Gradual increase of cut-on frequencies for increasing orders is clearly seen. A detailed analysis of dispersion curves can be found, e.g., in Ref. [3].

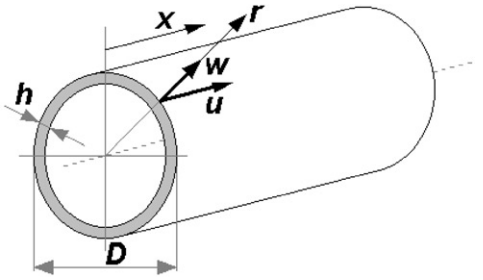

Fig. 3. Pipe geometry and displacement notation.

The analysis will concern pressure pulsation at lower frequencies. It can be thus restricted to axisymmetric motion in which the wall displacement in cylindrical co-ordinates $x-r$ can be split into orthogonal components u and w, Fig. 3.

2.2. Simplified solution

In this section the governing relationship for the acoustical pressure in the pipe will be given in terms of simple analytical formulae intended to allow the theoretical formulation of the analysis technique described in Section 3. The simple formulae, applicable only to frequencies well below the ring frequency, will be deduced from a complete solution describing the pipe behaviour in terms of acoustic waves in the contained fluid and vibration waves in the pipe wall.

While pressure pulsation in a fluid-filled pipe is produced by any type of wave (except by torsional waves as mentioned above), fluid waves which are of order $n = 0$ play a particular role in pipe acoustics as they are easiest to excite by fluid-borne sources. At frequencies well below the ring frequency the $n = 0$ mode is made up of fluid and longitudinal waves only. At these frequencies pressure pulsations are also excited by flexural waves, but the energy carried by these

pulsations is extremely low as the instantaneous pressure is linearly distributed over the cross-section about zero mean value.

Fig. 1 shows that, at lower frequencies, the $k-\omega$ dependence is approximately linear. The simplified relationship between the axial wave number and frequency for the mode $n=0$, applicable to pipes of high ring frequency, can be thus represented by

$$\kappa = ka = \varsigma\Omega, \tag{2}$$

with the proportionality coefficient ς equal to [9]

$$\varsigma_f = \frac{c_{s\infty}}{c_{f\infty}}\sqrt{1+\frac{2\eta+\upsilon^2}{1-\upsilon^2}\frac{c_{f\infty}^2}{c_{s\infty}^2}}, \quad \varsigma_s = \sqrt{1+\frac{\upsilon^2[(c_{s\infty}/c_{f\infty})^2-1]}{[(c_{s\infty}/c_{f\infty})^2-1](1-\upsilon^2)+2\eta+\upsilon^2}}, \quad \eta = \frac{\rho_f}{\rho_s}\frac{a}{h}, \tag{3}$$

where subscripts f and s refer to fluid and longitudinal (solid) waves, respectively. The speed of sound, either in fluid or wall, reads

$$\underline{c} = \frac{\omega}{k} = \frac{c_{s\infty}}{\varsigma}.$$

If the pipe is made of metal, the speed of sound in the fluid will be much smaller than that in the pipe wall, $c_{f\infty}^2 \ll c_{s\infty}^2$. The second term in the expression for ς_f will be thus insignificant unless the pipe wall is very thin making $\eta \gg 1$. This implies $\varsigma_f \approx c_{s\infty}/c_{f\infty}$ which in turn means that the speed of sound in the fluid of thick pipes will be close to that in an unbounded fluid, $c_{f\infty}$.

Since $0<\upsilon<0.5$ and $\eta>0$ the second term under the square root sign in the expression for ς_s, (2), is always smaller than unity. In most cases it will be much smaller than unity. This means that the speed of longitudinal waves will be little affected by the presence of fluid, staying very close to $c_{s\infty}$. The lower the Poisson ratio, the smaller the contribution of the second term. With υ approaching zero, i.e., in the absence of lateral contraction, this term vanishes.

2.3. *Pressure pulsation in pipes*

Fig. 4 shows a comparison between the exact and the approximate solution (2) of non-dimensional wave numbers of propagating waves corresponding to $n=0$. The approximate simple formula is seen to hold below $\Omega \approx 0.4$ (thin pipe) and $\Omega \approx 0.7$ (thick pipe) for fluid waves and below $\Omega \approx 0.7$ for longitudinal waves. These limits will usually satisfy most applications.

A more severe limiting factor where upper frequency limit is concerned will be the presence of higher order waves which become propagating at fairly low frequencies in pipes of low ring frequency. These waves will couple the internal pressure with wall motions, which will result in an interference between the $n=0$ waves and higher order waves. The present analysis is inapplicable to cases where higher order waves are present. It thus becomes necessary to identify the applicable frequency range, i.e., the cut-on frequencies of higher order waves.

The cut-on frequencies corresponding to waves of different order can be found by either exact or approximate computation. A simple approximate formula for the cut-on frequency of nth order wave reads [9]

$$\Omega_n^c = \frac{\omega_n^c a}{c_{s\infty}} \approx \frac{\beta n(n^2-1)}{\sqrt{1+n^2(1+\eta/n)+\beta^2(n^2-1)^2}}, \quad \beta = \frac{h}{2\sqrt{3}a}. \tag{4}$$

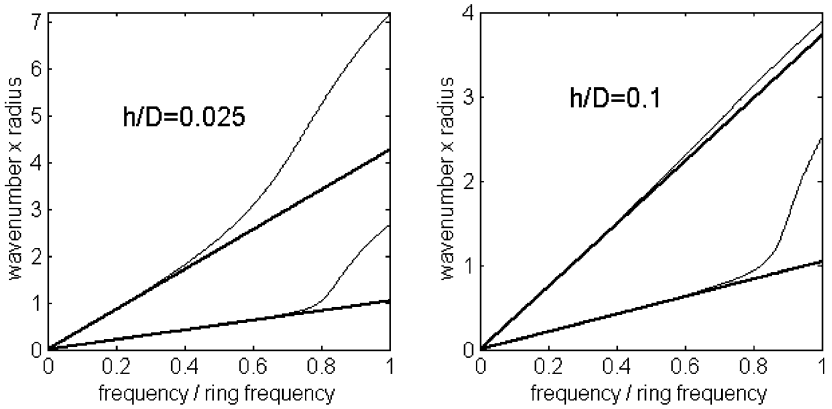

Fig. 4. Comparison of exact (thin line) and approximate (thick line) wave number solutions for zero order mode. Water-filled steel pipe, thickness/diameter $=\frac{1}{40}$ (left) and $\frac{1}{10}$ (right).

Upon neglecting the insignificant third term under the square root, the lowest non-zero cut-on frequency, that of $n = 2$ mode, becomes

$$\Omega_2^c = \frac{\omega_2^c a}{c_{s\infty}} \approx \frac{6\beta}{\sqrt{5+2\eta}} = \frac{h}{d}\sqrt{\frac{3}{5+\dfrac{\rho_f}{\rho_s}\dfrac{d}{h}}} < 0.775\frac{h}{d}, \quad d = 2a = D - h. \tag{4a}$$

The thinner the pipe and the heavier the fluid the lower will be the cut-on frequency. Fig. 5 shows the cut-on frequencies obtained by exact computation for steel pipes filled with: (a) light fluid—air compressed at 10 bar and (b) heavy fluid—water. Even a light fluid can make the first cut-on frequency descend well below 1 kHz if the wall thickness is small.

If the pipe analysis is done by experimental means, one can extract $n = 0$ mode out of total pipe motion by using a suitable array of transducers and an appropriate data processing. For example, the sum of signals coming from four transducers, either pressure or vibration sensitive ones, spaced equidistantly at the same axial position around the pipe circumference will be insensitive to $n = 1$ and 2 waves. In this way simple analysis of pipe pulsations can be extended to frequencies up to the cut on of the $n = 3$ mode. The upper frequency limit can be increased further still by using more transducers. If, however, the measurement in pipe is done without any special means to filter out undesirable modes of motion, then the upper frequency limit defined by (4a) should be respected.

It should be pointed out that the extracted $n = 0$ mode at frequencies below the first cut on will still contain all the waves belonging to this mode, i.e., two propagating ones—fluid and longitudinal—as well as evanescent waves. By choosing measurement positions away from the pipe ends, connections or discontinuities (half a wavelength or so), the contribution of evanescent waves will diminish. The influence of longitudinal waves will not diminish with distance; however, these waves will be as a rule very weakly coupled to the fluid and in most cases their effect on the measurement of pressure pulsations will be negligible, see Section 2.4. If this is not the case, some

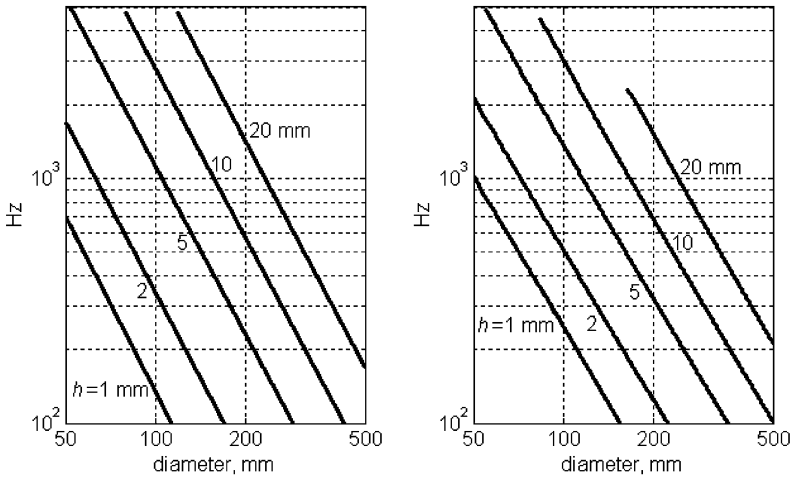

Fig. 5. First non-zero cut-on frequency, order $n = 2$, of a steel pipe filled with: left—light fluid (air compressed at 10 bar), right—heavy fluid (water).

complex transducer arrays can be used to separate longitudinal from acoustical waves, see e.g., Ref. [9].

One particular type of transducer seems suitable for the detection of pressure pulsation in pipes. This is a strain-sensitive wire wound around the pipe, first reported by Pinnington and Briscoe [19]. If the number of turns is an integer, then the strain in the pipe wall induced by the deformation will be proportional to the radial displacement of $n = 0$ mode only, which in turn is proportional to internal pressure pulsation.

2.4. *Influence of solid waves*

In the principal analysis, Section 3, it is assumed that the pressure pulsations propagate in the fluid at a unique speed of sound. As already pointed out, longitudinal waves will create pressure pulsations in the fluid which will add to the pulsations of fluid waves. As the sound speeds of the two waves are different, the analysis will be corrupted if the level of pulsations due to longitudinal waves becomes comparable to that of the fluid waves. In this section a simple analysis will be carried out to set-up a criterion for neglecting the influence of longitudinal waves.

One way to assess the contribution of the pressure induced by longitudinal waves p_s would consist of computing the level difference between this pressure and that due to fluid waves p_f at a given value of the ratio of energy flow in the fluid and in the pipe wall. It could be argued that p_s can be considered as negligible providing its level is much lower than that of p_f at energy flow equally partitioned between the fluid and the pipe wall. This argument is not more than intuitive, but in the absence of any concrete indication of pipe vibration and/or pressure levels it can serve as a rough guide not completely devoid of physical reality.

If more than one wave type propagates in the fluid, the fluid energy flow is not constant along the pipe, [6]. Part of the energy is exchanged between the wall and the fluid along the pipe at a rate

corresponding to the difference of the wave numbers of two waves. The total energy flow, being the sum of the two, remains constant (providing the dissipation losses are negligible as assumed).

As the energies in the fluid and the wall vary along the pipe, much as does the total acoustic pressure in the fluid, spatial averaging will be needed to get representative values of the two. For the sake of simplicity the averaging will be done over a hypothetically infinite pipe since averaging over a finite length would unnecessarily make the result dependent on details with little effect on the main findings.

In a general case, two waves, one fluid and one longitudinal, will simultaneously propagate in the $+x$ direction while two additional waves of the same type but different amplitudes will propagate in the $-x$ direction. The resulting acoustical pressure in the pipe will be the sum of four waves.

The spatially averaged levels of pressures p_f and p_s as well as the levels of energies in the fluid and the pipe wall are evaluated in the Appendix A. Eq. (A.7) gives the ratio of spatially averaged mean-square pressures induced by longitudinal and fluid waves as a function of the ratio of spatially averaged energy flows in the fluid and the pipe wall. This ratio is shown to be independent of frequency in the lower frequency range where the linear relationship (2) holds. The pressure ratio depends on the coefficient r, i.e., the ratio of amplitudes of oppositely propagating waves. If r is the same for longitudinal and fluid waves, the pressure ratio gets equal to the factor Φ, Eq. (A.7).

Fig. 6 shows the ratio of averaged pressures p_s and p_f, expressed in dB, for two cases: steel pipe filled with water (left) and steel pipe containing air at 10 bar static pressure (right). At equal level of fluid- and solid-borne energy flows (thick curve 0 dB) the level of pressure induced by f waves is much higher than that induced by s waves. In the case of water-filled pipe, the difference of levels of the two pressures is around 20 dB, getting even higher with the thickness-to-diameter ratio increasing towards values typical of most pipes. In the case of the air-filled pipe, the fluid-borne generated pressure is of much higher level than the solid-borne one, even at energies in the fluid much smaller than the energy in the wall. It can be concluded that wall vibrations of pipes containing light fluids, like gas, will not produce any noticeable effect on pressure pulsation in the

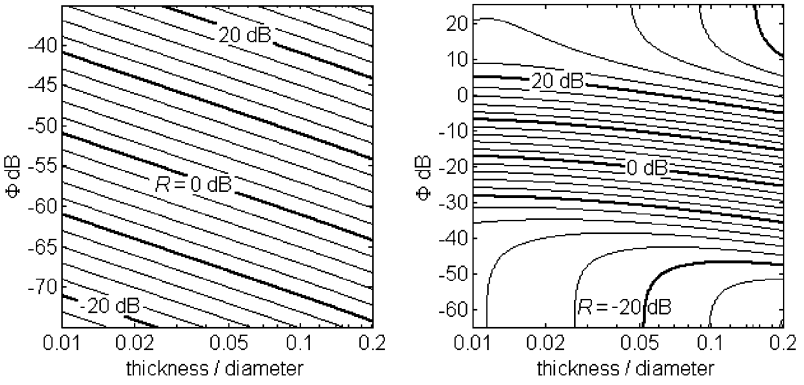

Fig. 6. Ordinate: dB level difference of pressure pulsations p_s and p_f due to longitudinal and fluid waves, expressed by the factor Φ, at different values of dB level difference of the solid- and fluid-borne acoustic powers. Steel pipe filled with: left—light fluid (air compressed at 10 bar), right—heavy fluid (water).

fluid. If however the fluid is heavy, the same condition requires that the energy in the pipe wall be smaller than the energy in the fluid.

3. Pipe analysis using invariant functions

In this section some simple techniques are described which provide potentially useful information about the pressure fluctuations in the pipe.

As this section deals exclusively with fluid waves, the subscript f used throughout Section 2 to indicate fluid-related quantities will be omitted. The pipe excitation is supposed to generate the pressure which originates from fluid-borne waves only. According to the findings in Section 2 this will occur always if the fluid is light, and in conditions of predominantly fluid-borne excitation if the fluid is heavy.

It will be assumed that the fluid is in steady motion. This condition makes the analysis more generally applicable and more accurate. The flow speed is supposed to be much smaller than the speed of sound in the fluid. The condition of fluid at rest will then be considered as a specific case to which the results of Section 3 will equally apply.

3.1. Basic relationships

Due to the fluid flow a Doppler shift will take place, making the wave numbers of fluid waves propagating in opposite directions unequal (bold symbols denote complex quantities)

$$\mathbf{p}(x) = \mathbf{A}_+ \mathrm{e}^{\mathrm{j}k_+ x} + \mathbf{A}_- \mathrm{e}^{\mathrm{j}k_- x}, \tag{5}$$

where

$$k_+ = \frac{\omega}{c+v} = \frac{k}{1+M}, \quad k_- = \frac{\omega}{c-v} = \frac{k}{1-M}, \quad k = \frac{\omega}{c},$$

M denoting the Mach number. By introducing a modified wave number k:

$$\frac{k}{1-M^2} \to k, \quad \text{i.e. } k_+ = k(1-M), \quad k_- = k(1+M).$$

Eq. (5) can be factorised by a term containing Mach number

$$\mathbf{p}(x) = \mathrm{e}^{\mathrm{j}kMx}(\mathbf{A}_+ \mathrm{e}^{-\mathrm{j}kx} + \mathbf{A}_- \mathrm{e}^{\mathrm{j}kx}). \tag{5a}$$

The pressure cross-spectrum between two points, x_a and x_b, is then obtained as follows:

$$\begin{aligned} \mathbf{S}_{ab} &= \mathbf{p}(x_a)^* \mathbf{p}(x_b) \\ &= \mathrm{e}^{\mathrm{j}kM(x_b - x_a)} \left(|\mathbf{A}_+|^2 \mathrm{e}^{-\mathrm{j}k(x_b - x_a)} + |\mathbf{A}_-|^2 \mathrm{e}^{\mathrm{j}k(x_b - x_a)} + 2\Re\left\{ \mathbf{A}_+ \mathbf{A}_-^* \mathrm{e}^{-\mathrm{j}k(x_b + x_a)} \right\} \right), \end{aligned} \tag{6}$$

where an asterisk denotes the complex conjugate and $\Re$ real part. Its power spectrum counterpart is simply obtained by setting $x_a = x_b$:

$$S_{aa} = \mathbf{p}(x_a)^* \mathbf{p}(x_a) = |\mathbf{A}_+|^2 + |\mathbf{A}_-|^2 + 2\Re\left\{ \mathbf{A}_+ \mathbf{A}_-^* \mathrm{e}^{-2\mathrm{j}kx_a} \right\}. \tag{6a}$$

By modifying the phase of the cross-spectrum proportionally with frequency as

$$\hat{\mathbf{S}}_{ab} = \mathbf{S}_{ab} \mathrm{e}^{\mathrm{j}kM(x_a - x_b)} \tag{7}$$

a modified cross-spectrum is obtained, denoted by a hat, representing physically the spectrum which would have been obtained if the observation points at x_a and x_b were moving relative to each other with the flow speed v. The moving cross-spectrum can be easily obtained by phase shifting the ordinary cross-spectrum by a function of the actual Mach number, as defined by Eq. (7). The moving cross-spectrum will be used in the remaining analysis.

It follows from Eq. (6) that the frequency-dependent quantity Θ,

$$\Theta_{ab} = \frac{\Im\left\{\hat{\mathbf{S}}_{ab}(x_a, x_b)\right\}}{\sin[k(x_a - x_b)]} = |\mathbf{A}_+|^2 - |\mathbf{A}_-|^2, \quad \Im\text{-imaginary part}, \tag{8}$$

is an invariant of space as the right-hand side part of Eq. (7) does not depend on x. In other words, the function Θ_{ab} remains the same whatever are the positions of points x_a and x_b. Being equal to the difference of amplitude squares of oppositely travelling fluid waves, it represents the scaled acoustic intensity of pressure pulsations W:

$$\Theta_{ab} = \rho c W. \tag{8a}$$

By combining cross- and power spectra, the real and imaginary parts of the amplitude cross product are obtained:

$$R = \Re\left\{\mathbf{A}_+\mathbf{A}_-^*\right\} = \frac{2\Re(\hat{\mathbf{S}}_{ab})\cos[k(x_a - x_b)] - S_{aa}\cos(2kx_b) - S_{bb}\cos(2kx_a)}{4\sin^2[k(x_a - x_b)]}, \tag{9a}$$

$$I = \Im\left\{\mathbf{A}_+\mathbf{A}_-^*\right\} = \frac{2\Re(\hat{\mathbf{S}}_{ab})\sin[k(x_a - x_b)] - S_{aa}\sin(2kx_b) - S_{bb}\sin(2kx_a)}{4\sin^2[k(x_a - x_b)]}. \tag{9b}$$

It turns out that the power spectrum at an arbitrary position x can be represented in terms of two new invariant functions, one real S_m and one complex $\mathbf{S}_v$:

$$S_{xx} = S_m + 2\ \Re\left\{\mathbf{S}_v \cdot \mathrm{e}^{-2\mathrm{j}kx}\right\} \tag{10}$$

which are simple linear combinations of R and I.

$$\begin{aligned} \mathbf{S}_v &= R + \mathrm{j}I \\ S_m &= |\mathbf{A}_+|^2 + |\mathbf{A}_-|^2 = S_{aa} - 2[R\cos(2kx_a) + I\sin(2kx_a)] \\ &= S_{bb} - 2[R\cos(2kx_b) + I\sin(2kx_b)]. \end{aligned} \tag{11}$$

The invariant S_m which is a real-valued function can be considered as a base spectrum of pressure pulsations. Its complement, the complex-valued invariant $\mathbf{S}_v$ can be considered as a modulation spectrum having the real and imaginary parts which oscillate along the pipe about zero mean value. These two functions can be used to predict pressure spectrum at any position x of the pipe, as seen by Eq. (10). In other words, once the two invariants S_m and $\mathbf{S}_v$ are identified, the pulsation spectrum is determined for all points of the pipe. This statement is valid as long as Eq. (5) is valid: in the section of the pipe considered there must be no sources or sinks or other phenomena, such as turbulence, which may make Eq. (5) invalid.

By inspecting Eqs. (8) and (9b) one can notice that ill-conditioning of the functions Θ, R and I will take place at frequencies where half the wavelength of sound in fluid becomes an integer fraction of the distance between the observation points x_a and x_b. This coincidence effect is a problem common to measurements in waveguides. It can be remedied by either taking the

ill-conditioned frequency parts of signals out of the analysis or suppressing the coincidence by adding one transducer and employing at each frequency a matched transducer combination which does not create singularities.

3.2. Speed of sound, flow velocity and spectral range

All of the invariant functions can be obtained by measuring pressure pulsations at two points on the pipe providing the sound speed and flow velocity are known. These values will rarely be known precisely. A technique described below enables the computation of the two parameters from experimental data.

Since Θ is invariant with respect to the positions of two observation points, the following function defined for three observation points x_a, x_b and x_c,

$$\mathrm{Z}_{abc} = \Im\{\hat{\mathbf{S}}_{ab}\}\sin[k(x_a - x_c)] - \Im\{\hat{\mathbf{S}}_{ac}\}\sin[k(x_a - x_b)], \tag{12}$$

should theoretically be zero at any frequency. The Z function contains two distinct variables: speed of sound in the fluid c, contained in the wave number k, and Mach number M, contained in the exponential term of the moving cross-spectrum.

To compute sound speed in the fluid and flow velocity the function Z_{abc} as defined by Eq. (12) is used. The values of sound speed c and Mach number M are considered as input parameters (7). Z_{abc} should theoretically vanish at all frequencies provided the true c and M are supplied. However, measurement imperfections and simplifications made in evaluating this function will never reduce it to zero at all frequencies simultaneously. One way to make a sensible estimate of c and M would thus be to integrate the absolute reciprocal of Z_{abc} across the effective frequency range of pressure pulsations $[\omega_1, \omega_2]$,

$$C(c, M) = \int_{\omega_1}^{\omega_2} \frac{\mathrm{d}\omega}{|Z_{abc}(\omega; c, M)|} \tag{13}$$

and find particular values c_0 and M_0 at which C is at maximum. This can be done by using an iteration procedure whereby c_0 and M_0 are given different values until a best fit of measurement data is found. The values of c_0 and M_0 identified in this way then represent the actual speed of sound and Mach number defined in the best-fit sense.

Initial values of sound speed can be determined from Eq. (3) and entered in a search loop which scans the range of sound speed and Mach number values to find the maximum of the cost function. Once c and v are found, the pressure field invariants can be readily computed by using Eqs. (9) and (11).

The base spectrum S_m equals the spatial average of pressure pulsations. This quantity will most efficiently characterize the pressure within the pipe in an average sense.

It follows from Eq. (10) that the admissible range of values of pressure spectrum at any frequency are given by

$$S_m - 2|\mathbf{S}_v| \leqslant S_{xx} \leqslant S_m + 2|\mathbf{S}_v|. \tag{14}$$

The last inequality specifies a spectral range which has to accommodate the pressure spectrum at any point along the pipe. It can be employed for a conservative prediction of the r.m.s. pressure in the pipe.

As S_m equals the sum of amplitude squares while Θ (defined by Eq. (8)) equals their difference, the mean-square spectra of the waves propagating in positive and negative directions, S_+ and S_- respectively, can be easily found from

$$S_+ = (S_m + \Theta)/2, \quad S_- = (S_m - \Theta)/2. \tag{15}$$

4. Measurements

By using Eqs. (3), (8), (9) and (12) a computer program was made in Matlab for pipe pressure analysis. It was then used on measurement data collected in two experiments described below.

4.1. Air-filled pipe

A few measurements were done on a ϕ27 mm, 2 mm thick steel pipe connected by a flexible hose to a vibrator cooler fan (Goodmans V50). The free end of the pipe had three flute-like holes which could be individually opened or closed to control the flow of air through the pipe; see Fig. 7. Three piezoelectric pressure transducers PCB 106B spaced by 120 mm were flush-mounted close to the pipe inlet. A four-channel FFT card OROS 25 connected to a PC was used for spectrum analysis.

Measurements were done in five regimes resulting from different combinations of open holes; see Table 1 (third hole was always kept closed). The fifth regime represents a particular case, that of zero fluid flow produced by fully closing the pipe.

Fig. 8 shows the r.m.s. spectrum of measured pressure pulsations in regime 2, energy averaged across three measurement positions. A peak at 700 Hz corresponds to the blade passing frequency of the fan. Fig. 9 shows the corresponding cost function C evaluated for the range of sound speed and flow velocity values. A distinct single peak is noticeable.

Fig. 10 shows the cost function for the first four regimes using the grey scale. The scale is normalized to 1, ranging from $\frac{1}{25}$ to 1 on graphs (a–c) and from $\frac{1}{18}$ to 1 on (d). The maximum, indicated by the crossing of the two dotted lines, shows the best-fit value for both the flow velocity and sound speed.

In parallel with the acoustic measurements, the flow velocity was estimated by using a hand-held anemometer, Testoterm 4400, complemented by an adapter to fit the holes and end opening. The temperature of the air inside the pipe was monitored by a small thermo probe. This enabled an estimation of sound speed in the pipe to be made.

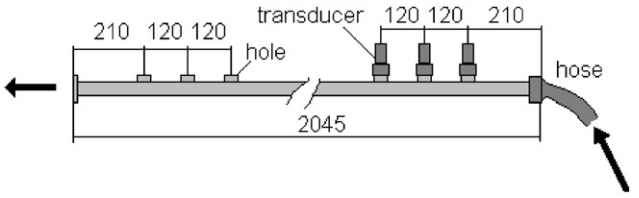

Fig. 7. Test rig scheme of air-filled pipe.

Table 1
Measurement regimes on air-filled pipe

Regime	End opening	Hole 1	Hole 2
1	C	O	C
2	C	C	O
3	C	O	O
4	O	C	C
5	C	C	C

C–closed, O–open.

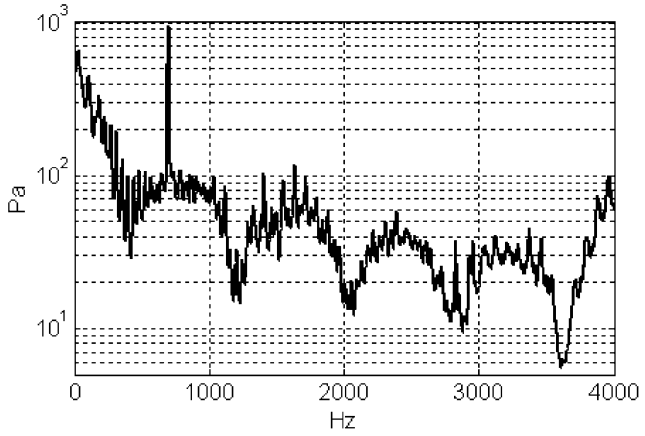

Fig. 8. Mean r.m.s. pressure spectrum S_m of air-filled pipe—regime 2.

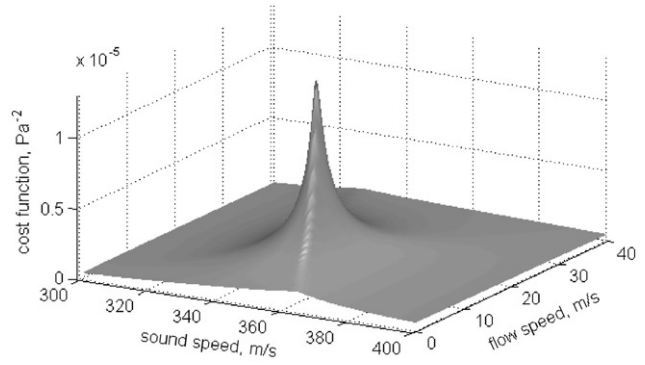

Fig. 9. Air-filled pipe: cost function C for the determination of sound speed and flow velocity obtained by measurements in regime 2.

Table 2 gives the comparison of two groups of measurements. The discrepancy in flow velocity measurement could be attributed to some extent to errors induced by the anemometric technique used. The overall matching achieved between the acoustical and traditional measurements is seen to be very good, indicating the robustness of the developed method.

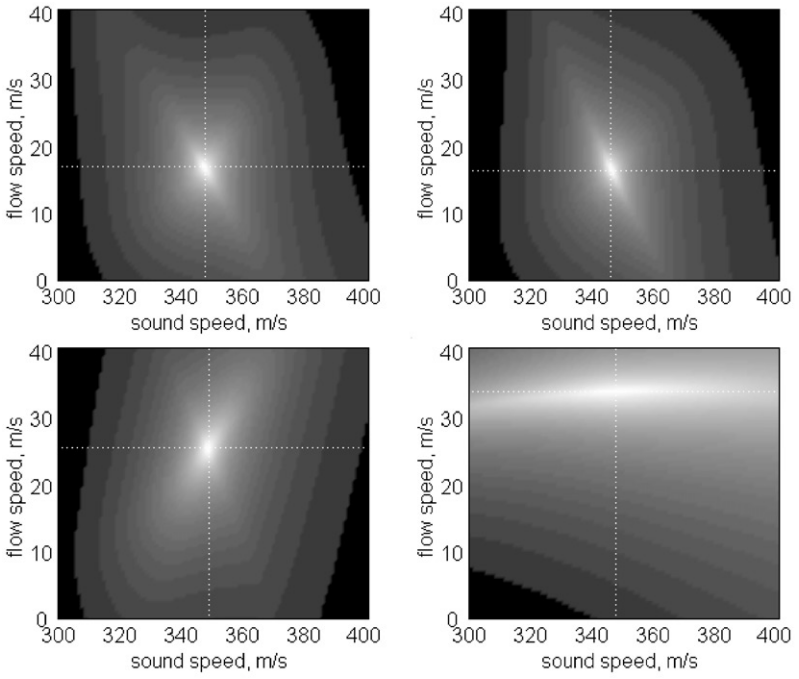

Fig. 10. Air-filled pipe: comparison of cost functions for regimes 1–4, clockwise from top left. Dotted lines indicate position of maximum. Extreme values: black 0.04 (0.055 for diagram 4); white 1.

Table 2
Comparison of measurement results on air-filled pipe

Regime	Temperature (°C)	Speed of sound via temperature readings (m/s)	Speed of sound via acoustic measurement (m/s)	Flow velocity via anemometer readings (m/s)	Flow velocity via acoustic measurement (m/s)
1	25	347	346	18	17
2	25	347	348	18	17.5
3	27	348	349	26	26
4	27	348	348	36	34.5

By looking at Eq. (8), one can see that the function Θ becomes more and more error sensitive the smaller the difference of the amplitudes of oppositely propagating waves. Thus, conditions close to total acoustic reflection in the pipe will unfavourably affect results. This can be seen in Fig. 11 which shows the C function plot for regime 5 where the pipe was fully closed. No distinct maximum can be seen, the C function pattern being unevenly spread all over the parameter range. In fact, the difference between maximum and minimum values of the cost function is in this case a trivial 3.6% which is an unusable value.

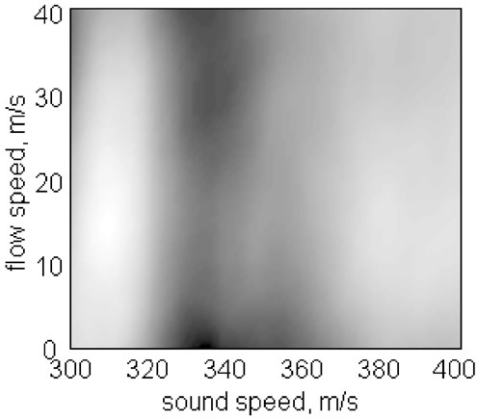

Fig. 11. Air-filled pipe: cost function of fully closed pipe, regime 5. Extreme values: black 0.964; white 1.

While the first three regimes, i.e., the ones with closed end opening, produced sharp maxima, regime 4 produced instead a fairly smeared arc peaking nevertheless at correct values of c and v. The reason for this peculiarity can be seen in Figs. 12(a) and (b): unlike in regimes 1–3, in regime 4 the difference of the amplitudes of positively and negatively propagating waves is small, thus ill conditioning the processing algorithm. The spectra in frequency bands around the coincidence frequencies, which at the transducer spacing of 0.12 m were at $\approx$1450 and $\approx$2900 Hz, were contaminated by errors and were consequently deleted from the processing.

4.2. *Liquid-filled pipe*

A ϕ33.5 mm, 3 mm thick steel pipe, part of a hydraulic test rig used for acoustic measurements, was equipped with flush mounted piezoelectric transducers (Kistler 7031). The water in the circuit was driven by a centrifugal pump. Two hydraulic anechoic tubes were inserted in front and at the rear of the measurement section to suppress pump noise,[1] see Fig. 13. The noise in the fluid was actually produced by a valve within the measurement section. As the flow velocity was small in comparison to sound speed, around 2 m/s, the value of the Mach number was set to 0.

The measurement array consisted of three transducers. A fourth transducer was mounted downstream about half a metre away. It provided a signal for comparison with the spectrum predicted by the measurement array according to Eq. (10).

Fig. 14 shows the r.m.s. pressure spectra measured by three array transducers (thin lines) and by the fourth control transducer (thick line). The spectrum at the fourth point was computed by using Eq. (10). As it closely matches the measured spectrum, it is not shown explicitly. Rather the

[1] The role of an anechoic tube is to suppress reflections of sound waves. Each anechoic tube consisted of a thin inner cylindrical perforated metallic tube enveloped by a thick flexible damped hose. This resonator device has a good absorption over a wide range of frequencies owing to the perforation rate continuously varying over the tube length.

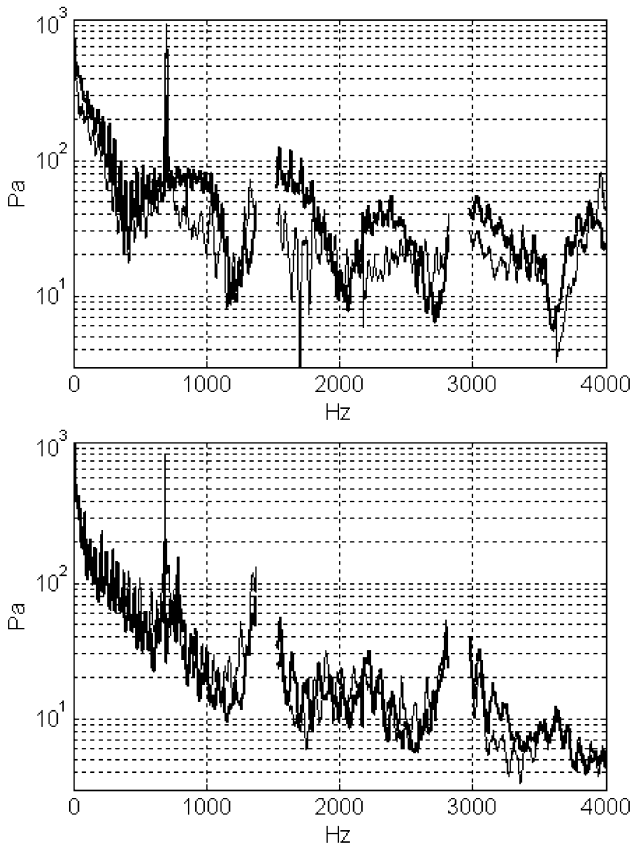

Fig. 12. Air-filled pipe: r.m.s. spectra of waves propagating towards pipe end (S_+, thick line) and from the end (S_-, thin line). Top: regime 2; bottom: regime 4.

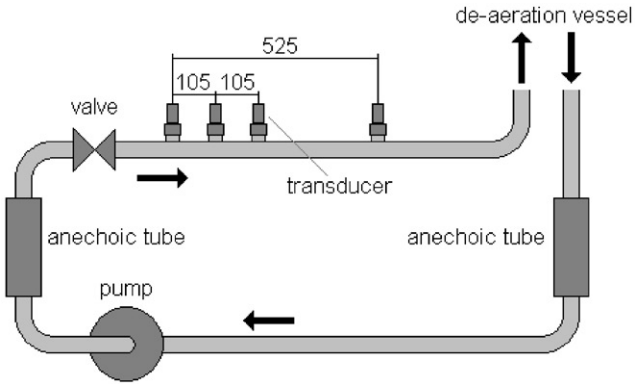

Fig. 13. Test rig scheme of water-filled pipe.

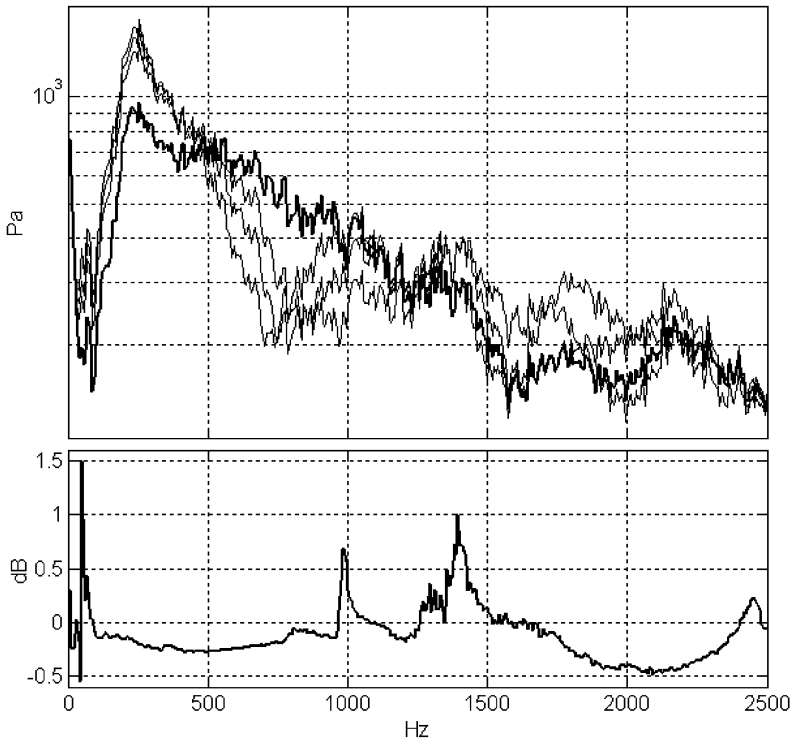

Fig. 14. Water-filled pipe: Top: r.m.s. pressure spectrum S_{xx} at three array transducers (thin lines) and the control transducer (thick line). Bottom: Difference between measured and predicted levels of r.m.s. pressure at the control transducer position.

difference in the levels of the two spectra is plotted at the lower part of Fig. 14 in dB scale. It can be seen that this difference rarely exceeds 0.5 dB which confirms the robustness of the spectrum recovery method.

Fig. 15 shows the base spectrum and the spectrum range obtained from Eqs. (11) and (14). At lower frequencies the difference between pressure maxima and minima can attain as much as 15–20 dB. The difference decreases with frequency, and the reason is seen in Fig. 16 which displays the spectra of positive and negative propagating pressure waves computed by using condition (15). The difference of the two which rises with frequency clearly indicates that absorption by the anechoic tubes increases with frequency which in turn reduces the r.m.s. pressure variations along the pipe axis.

5. Conclusions

Based on simplifications of an exact theoretical representation of the acoustic pressure pulsation transmission in pipes with flow, three invariant functions were evaluated. These functions can be obtained from three transducer measurements and can be used to used to

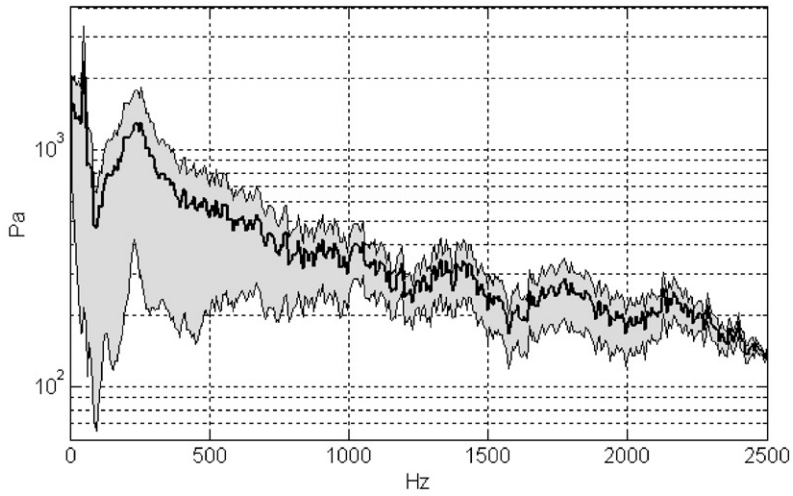

Fig. 15. Water-filled pipe: Base spectrum S_m—thick line. Shaded area represents spectral range applicable to the entire pipe.

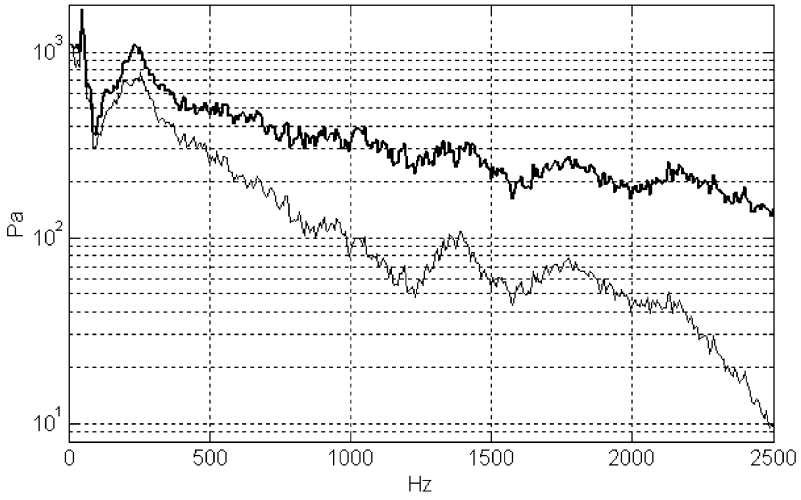

Fig. 16. Water-filled pipe: r.m.s. spectra of positive propagating (S_+, thick line) and negative propagating (S_-, thin line) pressure pulsation components.

determine: base pressure spectrum (spatial mean r.m.s. value), pressure maxima and minima, pressure spectrum at a defined position in pipe, speed of sound in the contained fluid, fluid flow velocity.

Measurements carried out on one air-filled and one water-filled pipe have demonstrated the potential of pipe invariant functions for acoustical analysis. In many cases the measurement of flow velocity by acoustical analysis will be possible.

The developed methodology is limited to frequencies which are well below the pipe ring frequency, i.e., where only simple waves can propagate. Expressions and diagrams given in Section 2 can help the reader to find out the permissible frequency range for each particular case.

The developed methodology may suffer from the influence of longitudinal vibrations of the pipe producing internal pressure which may adversely superimpose on pressure fluctuations initially of fluid-borne origin. This influence was found to be negligible in the case of a light fluid, but should be checked if a heavy fluid is contained in the pipe.

The method for experimental identification of field quantities uses three transducers only. As the developed method is basically an inverse one, singular frequencies exist at or close to which signal conditioning is poor. These frequencies are related to the geometry of transducer array. In order to avoid ill conditioning, an additional transducer may be used to provide better conditioning based on extra combination of signals.

Appendix A. Energy relationship between pressure of fluid and longitudinal waves

The pressure in the pipe due to fluid and longitudinal waves (temporal term omitted) reads

$$\mathbf{p}(x) = \mathbf{p}_f(x) + \mathbf{p}_s(x) = (\mathbf{P}_{f+}\mathrm{e}^{-\mathrm{j}k_f x} + \mathbf{P}_{f-}\mathrm{e}^{\mathrm{j}k_f x}) + (\mathbf{P}_{s+}\mathrm{e}^{-\mathrm{j}k_s x} + \mathbf{P}_{s-}\mathrm{e}^{\mathrm{j}k_s x}), \tag{A.1}$$

with $\mathbf{P}$ denoting complex pressure amplitudes and subscripts + and − denoting waves propagating in positive and negative directions. For the sake of simplicity the flow velocity is set to zero as it will not affect the results of this section providing the Mach number is low.

The spatially averaged mean-square value of the pressure will thus be

$$\langle \bar{p}^2 \rangle = \lim_{L\to\infty} \frac{1}{2L}\int_{-L}^{L} \bar{p}^2(x)\,\mathrm{d}x = \tfrac{1}{2}(|\mathbf{P}_{f+}|^2 + |\mathbf{P}_{f-}|^2 + |\mathbf{P}_{s+}|^2 + |\mathbf{P}_{s-}|^2),$$

with brackets denoting spatial average and overbars time average. By denoting the ratios of amplitudes of oppositely travelling waves by r, the space-averaged mean-square pressure becomes

$$\langle \bar{p}^2 \rangle = \tfrac{1}{2}\Big((1+r_f^2)|\mathbf{P}_{f+}|^2 + (1+r_s^2)|\mathbf{P}_{s+}|^2\Big) = \langle \bar{p}_f^2 \rangle + \langle \bar{p}_s^2 \rangle, \quad r = |\mathbf{P}_-/\mathbf{P}_+|. \tag{A.2}$$

The space-averaged intensity in the fluid, i.e., the real part of the product between the pressure and complex conjugate of fluid particle velocity $\mathbf{v}_f$, follows from Eqs. (A.1) and (A.2):

$$\begin{aligned} \mathbf{v}_f &= \frac{\mathrm{j}}{\omega\rho_f}\frac{\partial \mathbf{p}}{\partial x} \to \langle I_f \rangle = \tfrac{1}{2}\langle \Re(\mathbf{p}\cdot\mathbf{v}_f^*) \rangle \\ &= \frac{1}{2\rho_f c_{s\infty}}\Big[\zeta_f(1-r_f^2)\big|\mathbf{P}_{f+}\big|^2 + \zeta_s(1-r_s^2)|\mathbf{P}_{s+}|^2\Big], \end{aligned} \tag{A.3}$$

the asterisk denoting complex conjugate. It should be noted that $\boldsymbol{v}_f$ and I_f denote global fluid-borne quantities, i.e., such that are contributed by both f and s waves.

Likewise, the space-averaged intensity in the pipe wall, equal to the real part of the product between the axial stress σ and complex conjugate of axial velocity in the wall $\mathbf{v}_s$, will be

$$\boldsymbol{\sigma} = \frac{E}{1-\upsilon^2}\frac{\partial \boldsymbol{u}}{\partial x} \rightarrow \langle I_s \rangle = -\tfrac{1}{2}\langle \Re(\boldsymbol{\sigma}\cdot\mathbf{v}_s^*)\rangle$$
$$= \frac{Ec_{s\infty}\Omega^2}{2a^2(1-\upsilon^2)}[\zeta_f(1-r_f^2)|\mathbf{U}_{f+}|^2 + \zeta_s(1-r_s^2)|\mathbf{U}_{s+}|^2], \tag{A.4}$$

with $\mathbf{U}$ denoting the complex amplitude of axial wave displacement. Once again, v_s and I_s denote global solid-borne quantities.

The following relationship between the amplitudes of pressure and axial displacement, valid for either fluid or longitudinal waves, can be deduced from [9]

$$\frac{|\mathbf{U}|}{|\mathbf{P}|} = \frac{\Gamma}{\Omega}, \quad \Gamma = \frac{\upsilon a}{2\rho_f c_{s\infty}^2}H, \quad H = \frac{\zeta(c_{s\infty}^2/c_{f\infty}^2 - \zeta^2)}{\zeta^2 - 1}. \tag{A.5}$$

The energy flow is obtained by multiplying the intensity with the relevant section area:

$$\langle W_f \rangle = \pi(a-h)^2\langle I_f \rangle, \quad \langle W_s \rangle = 2\pi ah\langle I_s \rangle \tag{A.6}$$

By combining Eqs. (A.3)–(A.6) the desired relationship is obtained between the ratio of spatially averaged mean-square pressures due to longitudinal and fluid waves and the ratio of spatially averaged energy flows in the fluid and the pipe wall:

$$\frac{\langle \bar{p}_s^2 \rangle}{\langle \bar{p}_f^2 \rangle} = \frac{|1-r_f^2|(1+r_s^2)}{|1-r_s^2|(1+r_f^2)}\Phi, \tag{A.7}$$

where

$$\Phi = \frac{\zeta_f}{\zeta_s}\frac{GR - H_f^2}{H_s^2 - GR}, \quad R = \left|\frac{\langle W_s \rangle}{\langle W_f \rangle}\right|, \quad G = \frac{2}{\upsilon^2}\left(\frac{a}{h} - \frac{h}{a}\right)\frac{\rho_f}{\rho_s}. \tag{A.7a}$$

Energy flow can either be positive or negative. In the context of the present analysis the absolute value of energy flow is of concern, thus the appropriate notation in Eqs. (A.7) and (A.7a). As a consequence, Φ has to be always positive. Since $G > 0$ and $R > 0$, Eq. (A.7a) shows that this will hold only between certain boundaries of the energy ratio R:

$$\frac{H_f^2}{G} < R < \frac{H_s^2}{G}.$$

In other words, the energy cannot be shared by the fluid and the wall in an arbitrary way, but has to stay bounded within certain limits. In particular, energy in one of the two media cannot be zero.

References

[1] T.C. Lin, G.W. Morgan, Wave propagation through fluid contained in a cylindrical elastic shell, Journal of the Acoustical Society of America 28 (1956) 1165–1176.

[2] V.N. Merkulov, V.Yu. Prikhodko, V.V. Tytekin, Excitation and propagation of normal modes in thin fluid-filled elastic shells, Akustichesky Zhurnal 24 (1978) 723–730 (in Russian).

[3] C.R. Fuller, F.J. Fahy, Characteristics of wave propagation and energy distributions in cylindrical elastic shells filled with fluid, Journal of Sound and Vibration 81 (1982) 501–518.
[4] M. Möser, M. Heckl, K.-H. Ginters, On sound propagation in fluid-filled straight cylindrical pipes, Acustica 60 (1986) 34–44.
[5] Yu. Bobrovnitskii, V. Tyutekhin, Energy characteristics of composite waveguides, Akustichesky Zhurnal 32 (1986) 598–604 (in Russian).
[6] G. Pavić, Vibroacoustical energy flow in elastic circular cylindrical shells, Journal of Sound and Vibration 142 (1990) 293–310.
[7] J.W. Verheij, Multipath Sound Transfer from Resiliently Mounted Shipboard Machinery, Doctoral Thesis, Technische Physische Dienst TNO-TH, Delft, 1982.
[8] J.W. Verheij, Measurement of structure-borne wave intensity on lightly damped pipes, Noise Control Engineering Journal 35 (1990) 69–76.
[9] G. Pavić, Vibroacoustical energy flow through straight pipes, Journal of Sound and Vibration 154 (1992) 411–429.
[10] S. Bourget, F.J. Fahy, Vibrational power flow measurement along thin cylindrical pipe, Proceedings of the Fourth International Congress on Intensity Techniques, Senlis, France, 1993, pp. 153–157.
[11] C.A.F. de Jong, J.W. Verheij, Measurement of vibrational energy flow in straight fluid-filled pipes: a study of the effect of fluid–structure interaction. Proceedings of the Fourth International Congress on Intensity Techniques, Senlis, France, 1993, pp. 111–117.
[12] C.A.F. de Jong, Analysis of Pulsations and Vibrations of Fluid-filled Pipe Systems, Doctoral Thesis, Technische Physische Dienst TNO-TH, Delft, 1994.
[13] K. Trdak, Vibration and Acoustic Intensity in Pipes, Doctoral Thesis, Université de Technologie de Compiègne, 1995 (in French).
[14] L. Feng, Acoustic properties of fluid-filled elastic pipes, Journal of Sound and Vibration 176 (1994) 399–413.
[15] L. Feng, Experimental study of the acoustic properties of a finite elastic pipe filled with water/air, Journal of Sound Vibration 189 (1996) 511–524.
[16] G. Pavić, Analysis of acoustic pressure pulsations in pipes, Proceedings of Inter-Noise'97, Vol. 2, Budapest, 1997, pp. 1513-1518.
[17] AW. Leissa, Vibration of shells, National Aeronautics and Space Administration Report NASA SP-228, 1973, Chapter 2.
[18] W. Flügge, Stresses in Shells, 2nd Edition, Springer, Berlin, 1973.
[19] R.J. Pinnington, A. Briscoe, Externally applied sensor for axisymmetric waves in a fluid-filled pipe, Journal of Sound and Vibration 173 (1994) 503–516.